the FEBS Journal

The *Mycobacterium tuberculosis* ORF *Rv0654* encodes a carotenoid oxygenase mediating central and excentric cleavage of conventional and aromatic carotenoids

Daniel Scherzinger[1], Erdmann Scheffer[1], Cornelia Bär[1], Hansgeorg Ernst[2] and Salim Al-Babili[1]

1 Institute of Biology II, Albert-Ludwigs University of Freiburg, Germany
2 BASF Aktiengesellschaft, Fine Chemicals, and Biocatalysis Research, Ludwigshafen, Germany

Keywords
apocarotenoids; carotenoid cleavage oxygenase; carotenoids; lycopene; *Mycobacterium*; retinoids

Correspondence
S. Al-Babili, Institute for Biology II, Cell Biology, Albert-Ludwigs University of Freiburg, Schaenzlestrasse 1, D-79104 Freiburg, Germany
Fax: +49 761 203 2675
Tel: +49 761 203 8454
E-mail: salim.albabili@biologie.uni-freiburg.de

(Received 19 July 2010, revised 23 August 2010, accepted 8 September 2010)

doi:10.1111/j.1742-4658.2010.07873.x

Mycobacterium tuberculosis, the causative agent of tuberculosis, is assumed to lack carotenoids, which are widespread pigments fulfilling important functions as radical scavengers and as a source of apocarotenoids. In mammals, the synthesis of apocarotenoids, including retinoic acid, is initiated by the β-carotene cleavage oxygenases I and II catalyzing either a central or an excentric cleavage of β-carotene, respectively. The *M. tuberculosis* ORF *Rv0654* codes for a putative carotenoid oxygenase conserved in other mycobacteria. In the present study, we investigated the corresponding enzyme, here named *M. tuberculosis* carotenoid cleavage oxygenase (MtCCO). Using heterologously expressed and purified protein, we show that MtCCO converts several carotenoids and apocarotenoids *in vitro*. Moreover, the identification of the products suggests that, in contrast to other carotenoid oxygenases, MtCCO cleaves the central C15-C15′ and an excentric double bond at the C13-C14 position, leading to retinal (C_{20}), β-apo-14′-carotenal (C_{22}) and β-apo-13-carotenone (C_{18}) from β-carotene, as well as the corresponding hydroxylated products from zeaxanthin and lutein. Moreover, the enzyme cleaves also 3,3′-dihydroxy-isorenieratene representing aromatic carotenoids synthesized by other mycobacteria. Quantification of the products from different substrates indicates that the preference for each of the cleavage positions is determined by the hydroxylation and the nature of the ionone ring. The data obtained in the present study reveal MtCCO to be a novel carotenoid oxygenase and indicate that *M. tuberculosis* may utilize carotenoids from host cells and interfere with their retinoid metabolism.

Introduction

Mycobacterium tuberculosis, the causative agent of tuberculosis, is an intracellular human parasite infecting approximately two billion people and causing nine million new cases of tuberculosis and approximately two million deaths every year worldwide (http://www.who.int/gtb/). *M. tuberculosis cells* survive within the macrophages by preventing the phagosome maturation, which involves the fusion of phagosomes with lysosomes, and by avoiding the development of an appropriate immune response that could activate the host cell [1–5].

Several mycobacterial species are known to synthesize carotenoids [6], a group of isoprenoid pigments widely distributed in nature and generally composed of

Abbreviations
BCO, β-carotene cleavage oxygenase; MtCCO, *Mycobacterium tuberculosis* carotenoid cleavage oxygenase.

a C_{40}-polyene. These pigments exert a vital role as photoprotective pigments and free radical scavengers and represent essential components of the light-harvesting and reaction centre complexes of photosynthetic organisms [7–9]. In animals, carotenoids fulfill important functions, mainly as precursors of retinoids [e.g. retinal and vitamin A (retinol)] [10–12]. Retinal constitutes the visual chromophore of rhodopsins [13], whereas vitamin A and its derivative retinoic acid are involved in different processes, such as the immune response, development and reproduction [14,15]. Retro-retinoids represent a further group of vitamin A metabolites, including 14-OH-retroretinol and anhydroretinol, which were shown to affect general lymphocyte functions such as B-cell and T-cell proliferation [12,16]. In addition, cleavage products of the acyclic carotene lycopene (apolycopenals) are considered to have specific biological activities with respect to several cellular signalling pathways [17].

Retinoids belong to the apocarotenoids, a group of compounds arising through carotenoid cleavage generally catalyzed by carotenoid cleavage oxygenases, which are nonheme iron enzymes that target double bonds in carotenoid backbones, leading to aldehyde or ketone products [18–21]. However, some members of this enzyme family act on the interphenyl Cα-Cβ double bond of lignin [22] and other stilbene-derivatives such as resveratrol [23]. Retinal is formed through the symmetrical cleavage of β-carotene at the position C15-C15′ (Fig. 1), catalyzed by β-carotene cleavage oxygenase (BCO) I [24–26] in animals, and CarX and UmCco1 in the fungi *Fusarium fujikuroi* [27] and *Ustilago maydis* [28], respectively. In addition to BCOI, mammals contain a second carotenoid cleaving oxygenase, BCOII, that mediates the excentric cleavage of β-carotene at position C9′-C10′, leading to the C_{13}-compound β-ionone and β-apo-10′-carotenal (C_{27}) (Fig. 2) [29,30]. The BCO II product β-apo-10′ carotenal may lead to retinoic acid via β-oxidation-like reactions [31].

Several carotenoid oxygenases are known to cleave apocarotenoids instead of carotenoids [32–34]. For example, β-apo-10′-carotenal and several other apocarotenoids (e.g. β-apo-8′-carotenal and 3-OH-β-apo-10′-carotenal) (Fig. 2), represent precursors of retinal and its derivatives in the cyanobacteria *Synechocystis* and *Nostoc*, converted by the enzymes *Synechocystis*

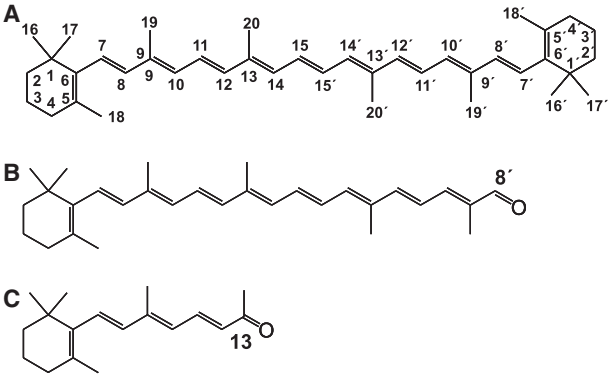

Fig. 1. Structure of β-carotene and selected apocarotenoids. The C_{40}-polyene of β-carotene (**A**) constitutes two β-ionone rings. Apocarotenoids are designated according to the cleavage site (atom numbers are depicted) [e.g. oxidative cleavage of the C8′-C7′ or the C13-C14 double bond leads to β-apo-8′-carotenal (**B**) or β-apo-13-carotenone (**C**), respectively]. Hydroxylation at the C3/C3′ positions leads to zeaxanthin from β-carotene and to lutein from α-carotene, an isomer of β-carotene containing one β- and one ε-ionone ring. Aromatic carotenoids (e.g. isorenieratene) contain ϕ-rings (Fig. 2).

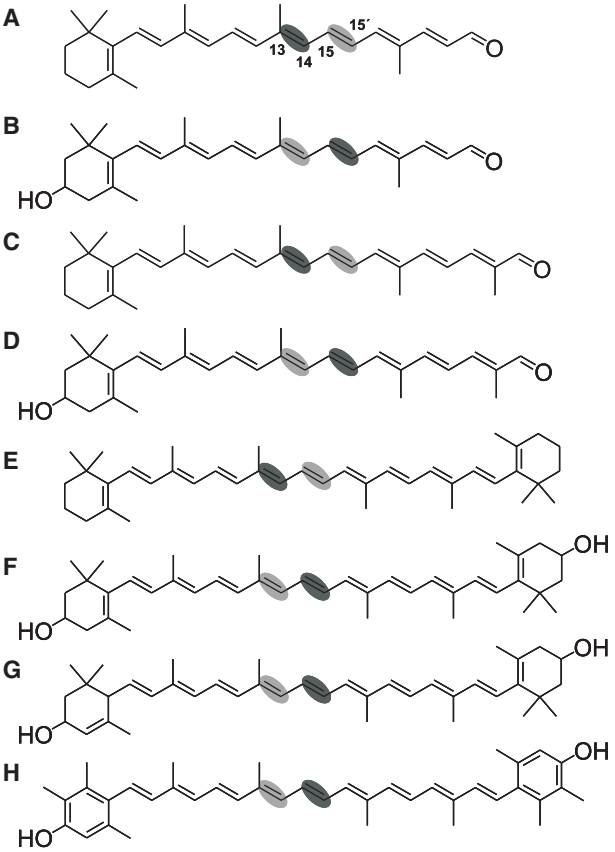

Fig. 2. Cleavage sites and structures of the substrates. The structures correspond to β-apo-10′-carotenal (C_{27}; **A**), 3-OH-β-apo-10′-carotenal (C_{27}; **B**); β-apo-8′-carotenal (C_{30}; **C**); 3-OH-β-apo-8′-carotenal (C_{30}; **D**); β-carotene (**E**); zeaxanthin (**F**); lutein (**G**) and 3,3′-dihydoxy-isorenieratene (**H**). The substrates were cleaved at the C13-C14 and the C15-C15′ double bonds. Preferred and less targeted sites are shaded in dark and light gray, respectively. The preference of the enzyme is deduced from the values presented in Table 2.

apocarotenoid cleavage oxygenase (formerly named as Diox1) and *Nostoc* apocarotenoid cleavage oxygenase [31,32]. In addition, apo-10′-carotenal is converted by the plant carotenoid cleavage dioxygense 8 [34,35] into the C_{18}-ketone β-apo-13-carotenone (Fig. 1) in the pathway leading to strigolactones, which act as plant hormones [36–38] and signalling molecules, attracting both symbiotic arbuscular mycorrhizal fungi and parasitic plants [39,40].

M. tuberculosis is considered to lack carotenoids, in contrast to the near relative *Mycobacterium marinum*. Indeed, the genes required for carotenoid biosynthesis have disappeared from *M. tuberculosis* during its evolution, which was accompanied by a reduction of the genome size [41]. Hence, it is unexpected that the *M. tuberculosis* genome H37Rv [42] still contains two ORFs (i.e. *Rv0654* and *Rv0913c*) coding for putative carotenoid cleavage oxygenases, indicating the capability to convert these pigments. In the present study, we report the characterization of the *Rv0654* encoded enzyme, which we refer to as the *M. tuberculosis* carotenoid cleavage oxygenase (MtCCO), as suggested by *in vitro* and *in vivo* studies.

Results

MtCCO cleaves apocarotenals at two different sites

Sequence comparisons suggested that MtCCO is a member of the carotenoid oxygenase family, showing approximately 44% similarity to the characterized enzyme *Nostoc* carotenoid cleavage dioxygenase [43] and containing the conserved four histidins residues required for binding of the cofactor Fe^{2+} [44] (Fig. S1). To determine its enzymatic activities, MtCCO was expressed in *Escherichia coli* cells as a glutathione *S*-transferase fusion protein, and the protein was purified using glutathione sepharose and released by the protease Factor X_a (Fig. S2). Using purified enzyme, we tested the C_{27}-compound β-apo-10′-carotenal (Fig. 2) known to be a suitable substrate for different carotenoid oxygenases [32–34,45]. In addition, we performed incubations with the stilbene derivative resveratrol cleaved by some members of the carotenoid oxygenase family [23], and the isoprenoids cholecalciferol (vitamin D_3), phylloquinone (vitamin K_1) and α-tocopherol, which contain double bonds that might be targeted by cleavage oxygenases. HPLC analyses of the *in vitro* assays did not show any cleavage of the noncarotenogenic substrates (data not shown). By contrast, β-apo-10′-carotenal was converted into β-apo-13-carotenone (C_{18}) (Fig. 3; I), as suggested by comparison with an authentic standard (Fig. 3; I) and LC-MS analysis (data not shown). This result indicated the cleavage of the C13-C14 double bond (Fig. 3). Pointing to the C15-C15′double bond as a second, less targeted cleavage site, incubation with β-apo-10′-carotenal led also to minor amounts of β-apo-15-carotenal (retinal; C_{20}) (Fig. 3, I).

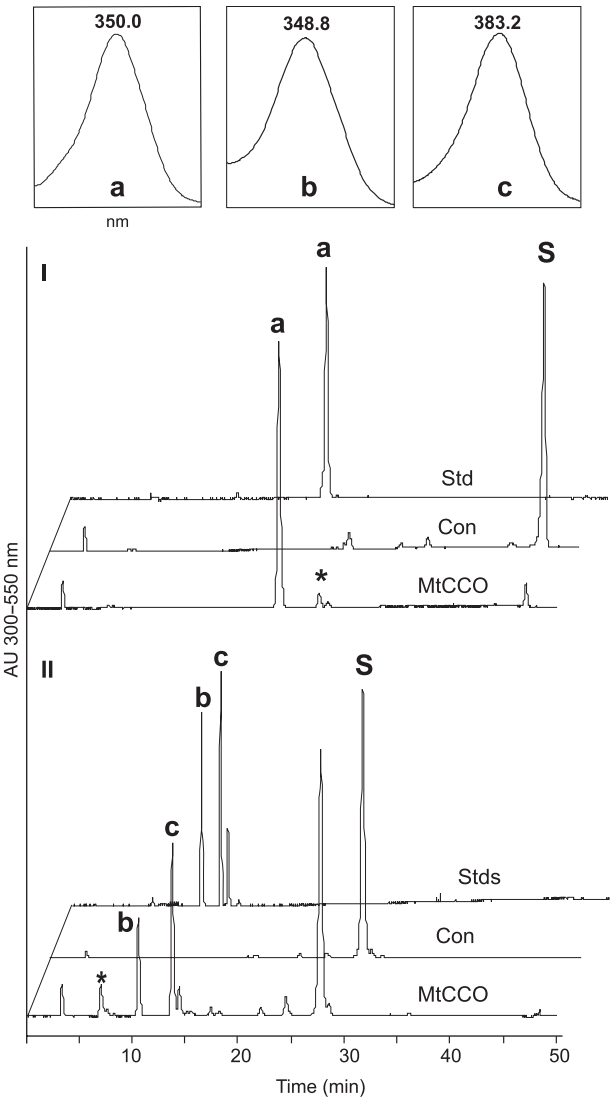

Fig. 3. HPLC analyses of *in vitro* assays with apocarotenoids. I: HPLC analyses of the incubation with β-apo-10′-carotenal (**S**) showed the conversion into β-apo-13-carotenone (**a**; C_{18}) identified by comparison with the authentic standard (Std). In addition, traces of retinal (*) were detected. II: The incubation of MtCCO with 3-OH-β-apo-10′-carotenal (**S**) led to the formation of 3-OH-β-apo-13-carotenone (**b**; C_{18}) and 3-OH-retinal (**c**; C_{20}). The products were identical to authentic standards (Stds; **b**, **c**) in their UV-visible spectra (insets) and elution characteristics. The chromatogramm (MtCCO) shows also the formation of a minor product (*).

To determine the effect of β-ionone ring modifications on the cleavage activity, MtCCO was incubated with 3-OH-β-apo-10′-carotenal (Fig. 2). As shown in the HPLC analysis (Fig. 3, II), 3-OH-β-apo-10′-carotenal was converted into 3-OH-β-apo-13-carotenone (C_{18}) and 3-OH-β-apo-15-carotenal (3-OH-retinal; C_{20}), besides a minor product presumably representing 3-OH-β-apo-11-carotenal (C_{15}). The C_{18} and the C_{20} products were identified by comparison with authentic standards (Fig. 3; II) and by LC-MS analyses (data not shown). These data suggested that MtCCO cleaves 3-OH-β-apo-10′-carotenal at two different sites, namely the C13-C14 and the C15-C15′ double bonds.

In a further approach, MtCCO was incubated with apocarotenoids of a longer chain length, namely the C_{30}-compunds β-apo-8′- and 3-OH-β-apo-8′-carotenal (Fig. 2). HPLC analysis (data not shown) of these incubations revealed the formation of β-apo-13-carotenone and retinal from β-apo-8′-carotenal and the corresponding hydroxylated derivatives from 3-OH-β-apo-8′-carotenal, confirming the cleavage of the C13-C14 and C15-C15′ double bonds in both substrates. Incubation of apocarotenoids shorter than β-apo-10′-carotenal [i.e. β-apo-12′- (C_{25}) β-apo-14′- (C_{22}), β-apo-15′-carotenal (retinal; C_{20}) and β-apo-15′-carotenoic acid (retinoic acid; C_{20})] revealed only weak activity with the C_{25}-compound, whereas substrates with a shorter chain length were not converted (data not shown). These results indicate that the β-apocarotenoids converted by MtCCO must have a chain length of at least C_{25}.

To shed light on the preference of MtCCO with respect to chain length and hydroxylation of the substrates, kinetic analyses were performed with the β-apo-8′- (C_{30}) and β-apo-10′-carotenal (C_{27}), as well as their hydroxylated derivatives, 3-OH-β-apo-8′- and 3-OH-β-apo-10′-carotenal. Table 1 gives the K_m and k_{cat} values determined in the biphasic incubation system used; see also Table S1 and Fig. S3. The lowest K_m was obtained for β-apo-8′-carotenal, followed by 3-OH-β-apo-8′-carotenal and β-apo-10′-carotenal and, finally, by 3-OH-β-apo-10′-carotenal. However, β-apo-8′-carotenal showed a lower k_{cat} value compared to 3-OH-β-apo-8′-carotenal. Although less pronounced, a similar tendency was also observed with the C_{27}-compounds. These data indicated that MtCCO exhibits higher affinities to unsubstituted apocarotenoids but converts their hydroxylated derivatives faster.

Table 1. K_m and k_{cat} values of MtCCO for different substrates. Each value represents the mean ± SD of three independent experiments.

Substrate	k_{cat} (s^{-1})	K_m (μM)
β-apo-8′-carotenal	392.7 ± 0.00	4.15 ± 0.68
β-apo-10′-carotenal	561.7 ± 27.62	29.36 ± 3.2
3-OH-β-apo-8′-carotenal	1307.6 ± 64.46	21.90 ± 2.6
3-OH-β-apo-10′-carotenal	764.3 ± 55.25	43.81 ± 5.5

MtCCO mediates a novel cleavage reaction of C_{40}-carotenoids

To further explore its substrates, purified MtCCO was incubated with β-carotene under the same conditions used for *in vitro* assays with apocarotenoids. However, only traces of activity were observed in the subsequent HPLC analysis. Therefore, we applied a higher enzyme concentration and prolonged incubation times. These improved conditions resulted in the accumulation of three different products (Fig. 4, I) identified by their chromatographic behaviour and LC-MS analyses (data not shown) as β-apo-13-carotenone (C_{18}), β-apo-15′-carotenal (retinal, C_{20}) and β-apo-14′-carotenal (C_{22}). This activity demonstrated that MtCCO mediates the symmetrical cleavage of β-carotene at the C15-C15′ site, as well as the asymmetrical cleavage of the C13-C14 or the C13′-C14′ double bond.

To test the cleavage of hydroxylated C_{40}-carotenoids, purified enzyme was incubated with zeaxanthin and lutein (Fig. 2) under the conditions used for β-carotene. As shown in Fig. 4 (II), zeaxanthin was converted to the 3-hydroxylated counterparts of the products obtained from β-carotene [i.e. 3-OH-β-apo-13-carotenone (C_{18}), 3-OH-β-apo-15′-carotenal (3-OH-retinal, C_{20}) and 3-OH-β-apo-14′-carotenal (C_{22})], which were confirmed by LC-MS analyses (data not shown). In addition, a minor product was detected, which may correspond to 3-OH-β-apo-11-carotenal (C_{15}).

The composition of the products formed from lutein was more complicated as a result of the presence of two different ionone rings (i.e. ε and β) (Fig. 2). As shown in Fig. 4 (III), four major and two minor products were detected in the corresponding HPLC analysis. On the basis of UV-visible spectra and elution patterns, the two major products, $\mathbf{h_2}$ and $\mathbf{h_1}$, were identified as 3-OH-β-apo-15′-carotenal (3-OH-retinal, C_{20}) and its almost co-eluting isomer with lower absorption maximum 3-OH-α-apo-15′-carotenal, respectively. The other two major products, **g** and **i**, were assumed to be 3-OH-α-apo-13-carotenone (C_{18}) and 3-OH-β-apo-14′-carotenal (C_{22}), respectively. This assumption was supported by the shorter retention time and the lower UV-visible absorption maximum of product g compared to 3-OH-β-apo-13-carotenone formed from

zeaxanthin (product **d**; Fig. 4, II). To confirm their identities, the four major products obtained from lutein were purified and applied to LC-MS analyses. As shown in Fig. 5, the products **g**, $\mathbf{h_1}$, $\mathbf{h_2}$ and **i** exhibited the expected molecular ions $[M+H]^+$ of *m/z* 275, 301, 301 and 327, respectively. The LC-MS analyses also showed fragments corresponding to the respective $[M+H\text{-}H_2O]^+$ ions, which were more abundant in the analyses of the α- than in those of the β-compounds (data not shown).

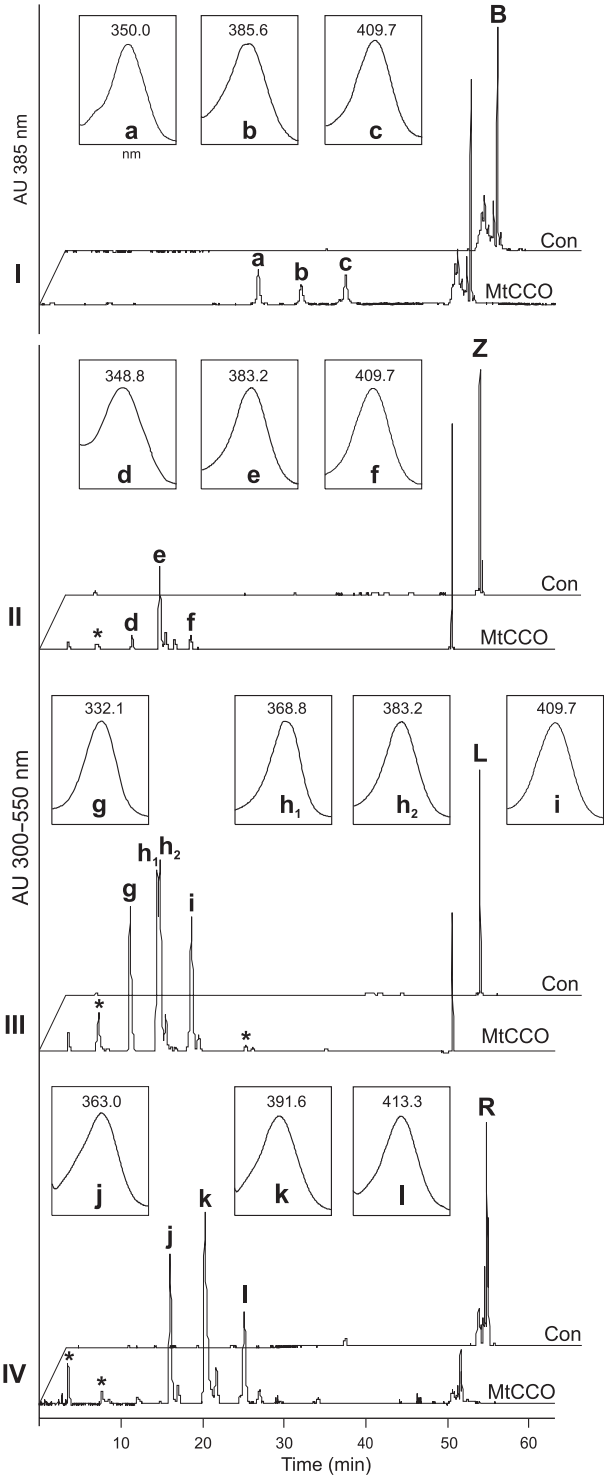

Several mycobacterial species, other than *M. tuberculosis*, accumulate specific carotenoids (i.e carotenoids with phenolic end groups) [6]. Because MtCCO represents a subfamily of mycobacterial carotenoid cleavage oxygenases (Fig. S4), we tested its activity on the aromatic carotenoid 3,3′-dihydroxy-isorenieratene (3,3′-dihydroxy-ϕ, ϕ-carotene) (Fig. 2). As shown in Fig. 4, IV, this substrate was readily converted into three major products, **j**, **k**, **l**, besides two minor compounds. On the basis of their chromatographic properties, we assumed that the three major products, **j**, **k** and **l**, correspond to 3-OH-φ-apo-13-carotenone (C_{18}), 3-OH-ϕ-apo-15′-carotenal (C_{20}) and 3-OH-ϕ-apo-14′-carotenal (C_{22}), respectively. To confirm this assumption, the three products were purified and subjected to LC-MS analyses (Fig. 6), which revealed the expected $[M+H]^+$ molecular ions of *m/z* 271 (product **j**), 297 (product **k**) and 323 (product **l**).

The site preference of MtCCO is determined by hydroxylation and structure of the ionone ring

In vitro incubations suggested the cleavage of two different sites (i.e. the C15-C15′ and C13-C14 double bonds). However, the different amounts of the corresponding products indicated that the two double bonds are not equally targeted among the substrates tested. Aiming to determine the enzyme's preference, the relative amounts of the C_{18}, C_{22} and C_{20} products of three independent incubations were investigated. The obtained values (Table 2) indicated that the preference of the enzyme is highly affected by the presence of the 3-hydroxy-modification in the β-ionone ring. For example, 80% and 97% of the total product amounts

Fig. 4. HPLC analyses of the incubations of MtCCO with different carotenoid substrates. UV-visible spectra of the products are shown in the insets. I: Incubation with β-carotene (**B**) leading to β-apo-13-carotenone (**a**; C_{18}), retinal (**b**; C_{20}) and β-apo-14-carotenal (**c**; C_{22}). II: Incubation with zeaxanthin (**Z**) showing the formation of 3-OH-β-apo-13-carotenone (**d**; C_{18}), 3-OH-retinal (**e**; C_{20}) and 3-OH-β-apo-14-carotenal (**f**; C_{22}). III: Incubation with lutein (**L**) leading to the supposed products 3-OH-α-apo-13-carotenone (**g**; C_{18}), 3-OH-α-apo-15′-carotenal ($\mathbf{h_1}$; C_{20}), its isomer 3-OH-β-apo-15′-carotenal (3-OH-retinal; $\mathbf{h_2}$) and 3-OH-β-apo-14-carotenal (**i**; C_{22}). IV: Incubation with 3,3′-dihydoxy-isorenieratene (**R**) showing the formation of tentative C_{18}- (**j**), C_{20}- (**k**) and C_{22}-products (**l**). In II, III and IV, traces of other unidentified products (*) were also detected.

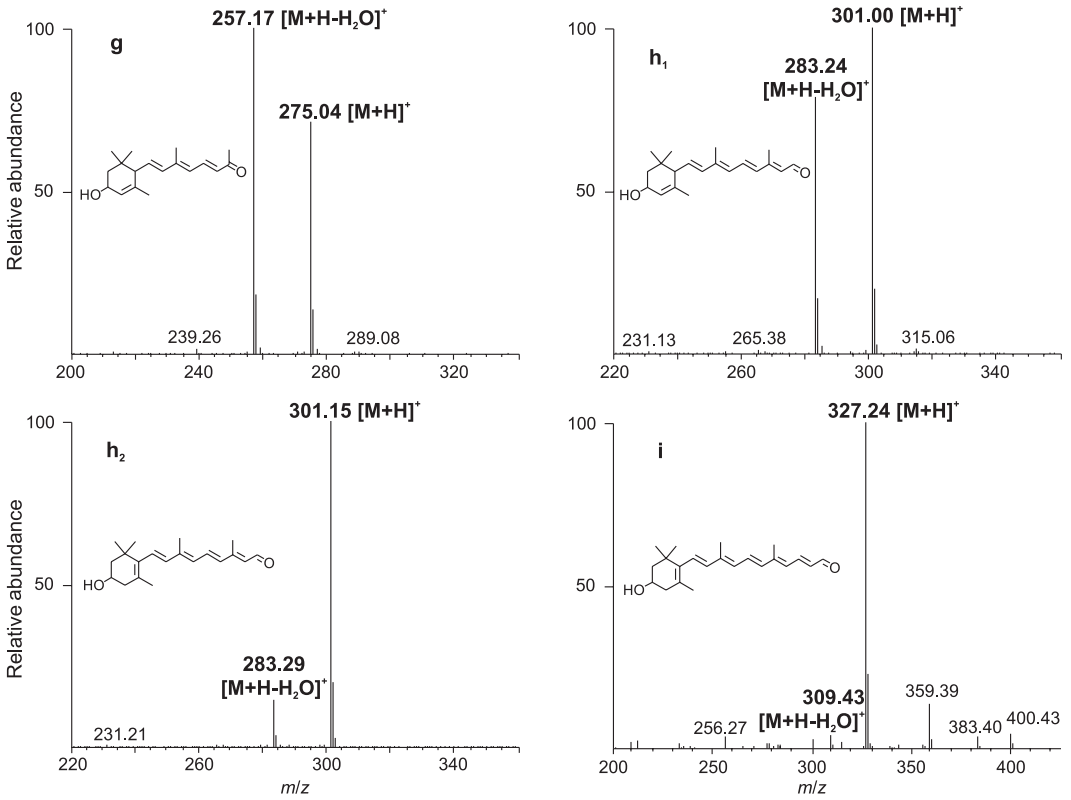

Fig. 5. LC-MS analyses of the lutein cleavage products. The cleavage products of the incubation with lutein were purified by HPLC and subjected to LC-MS analyses. The products showed the molecular ions $[M+H]^+$ of *m/z* 275 (**g**), *m/z* 301 (**h_1** and **h_2**) and *m/z* 327 (**i**), which are expected for 3-OH-α-apo-13-carotenone (C_{18}), 3-OH-α-apo-15′-carotenal (C_{20}), 3-OH-β-apo-15′-carotenal (C_{20}; 3-OH-retinal) and 3-OH-β-apo-14′-carotenal (C_{22}), respectively. The structures of the products are depicted. The spectra of the products with an α-ionone ring exhibited pronounced $[M+H-H_2O]^+$ fragment ions.

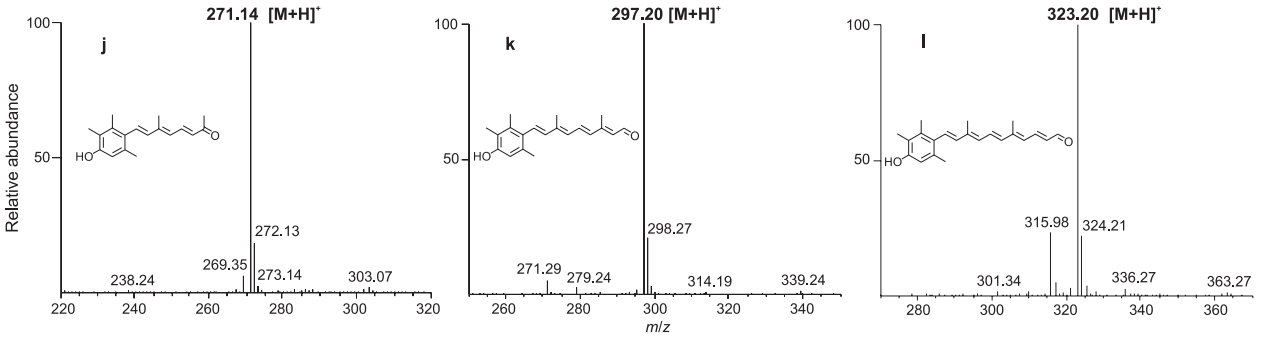

Fig. 6. LC-MS analyses of the 3,3′-dihydroxy-isorenieratene cleavage products. The purified products were subjected to LC-MS analyses and identified as 3-OH-ϕ-apo-13-carotenone (C_{18}; **j**), 3-OH-ϕ-apo-15′-carotenal (C_{20}; **k**) and 3-OH-ϕ-apo-14′-carotenal (C_{22}; **l**), as suggested by the expected molecular ions $[M+H]^+$ of *m/z* 271 (**j**), *m/z* 297 (**k**) and *m/z* 323 (**l**), respectively. Structures shown correspond to the products.

obtained from β-apo-8′-β-apo-10′-carotenal, respectively, were identified as β-apo-13-carotenone (C_{18}) arising through the C13-C14 cleavage, whereas the C3-hydroxylated counterparts were mainly targeted at the C15-C15′ site, as suggested by the relative higher amounts of 3-OH-retinal (C_{20}). Similarly, the relative amounts of the C_{18} and C_{22} products resulting from the cleavage of C13-C14 (or C13′-C14′) in β-carotene were much higher than those of the corresponding hydroxylated products formed from zeaxanthin. This

Table 2. Cleavage Specificity of MtCCO. The ratios of products resulting from the cleavage at the C13-C14/C13′-C14′ (C_{18} and C_{22}) and at the C15-C15′ (C_{20}) double bonds are shown, relative to the total amount of both product types. The values were calculated from the product peak areas of a MaxPlot 300–550 nm of the respective HPLC analyses.

Substrate	C13-C14/ C13′-C14′ (%)	C15-C15′ (%)
β-apo-8′-carotenal	79.6 ± 1.4	20.4 ± 1.3
β-apo-10′-carotenal	97.0 ± 4.6	3.0 ± 0.8
β-carotene	86.0 ± 13.8	14.0 ± 4.5
3-OH-β-apo-8′-carotenal	5.0 ± 0.1	95.0 ± 2.3
3-OH-β-apo-10′-carotenal	30.5 ± 0.6	69.5 ± 1.3
Zeaxanthin	17.1 ± 8.3	82.9 ± 4.9
Lutein	45.6 ± 1.7	54.4 ± 0.2
3,3′-dihydoxy-isorenieratene	45.7 ± 11.5	54.3 ± 3.9

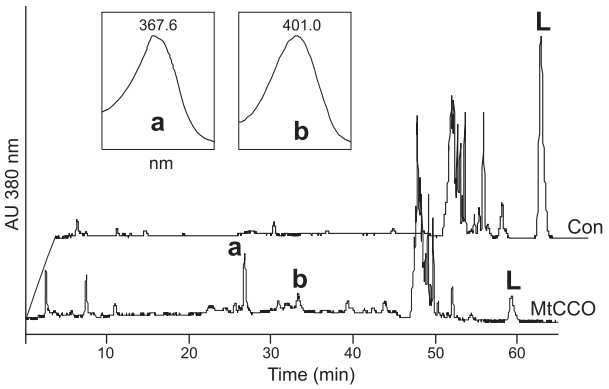

Fig. 7. Expression of MtCCO in lycopene accumulating *E. coli* cells. HPLC analyses of lycopene (**L**) accumulating *E. coli* cells expressing a thioredoxin-MtCCO fusion protein (MtCCO) or thioredoxin (Con). The activity of MtCCO resulted in the formation of two products identified as apo-13-lycopenone (**a**; C_{18}) and apo-15′-lycopenal (acycloretinal; **b**; C_{20}). The nature of the products was deduced from the UV-visible spectra (insets) and elution patterns.

indicated that the occurrence of the 3-hydroxy-group favours the symmetrical cleavage at the C15-C15′ double bond. However, this preference is attenuated if the substrates contain an ε- or a ϕ-ionone ring, as deduced from the incubations with lutein and 3,3′-dihydroxy-isorenieratene. Moreover, the asymmetrical cleavage of lutein appeared to occur only at the C13-C14 site adjacent to the ε-ionone ring, and not at the C13′-C14′ on the β-ionone site, as indicated by the absence of β-apo-13-carotenone in the corresponding analyses.

MtCCO cleaves lycopene *in vivo*

In vitro incubations with the acyclic substrate lycopene did not lead to any detectable conversion, most likely as a result of the high hydrophobicity hindering solubilization with octyl-β-glucoside used for other substrates. Therefore, we tested the cleavage of lycopene *in vivo*. Accordingly, MtCCO was expressed as a thioredoxin-fusion in a lycopene-accumulating *E. coli* strain. Although the decolorization indicated a high conversion of the substrate, HPLC analyses of the cells showed only traces of two products (Fig. 7). On the basis of UV-visible spectra and elution pattern, the two products were identified as apo-13-lycopenone (C_{18}; **a**) and apo-15′-lycopenal (acycloretinal, C_{20}; **b**). These data indicated that MtCCO cleaves carotenoids *in vivo*.

Discussion

The biological relevance of carotenoid oxygenases in mycobacteria is mirrored by their common presence in the corresponding sequenced genomes available from the NCBI public database (http://www.ncbi.nlm.nih.gov/genomes), with the exception of the extremely reduced *Mycobacterium leprae* genome. These enzymes occur independently of the ecotype and the genome size (Fig. S4). They are encoded in the 7 Mb genome of *Mycobacterium smegmatis* str. MC2 155, in the reduced 4.4 Mb genome of the intracellular human parasite *M. tuberculosis*, as well as in the 6 Mb genome of *Mycobacterium* sp. JLS isolated from creosote-contaminated soil [46]. The number of the carotenoid oxygenases varies among mycobacterial species, ranging from one in *Mycobacterium abscessus* to three in *Mycobacterium avium* and *Mycobacterium vanbaalenii* (Fig. S4). The genome of *M. tuberculosis* H37Rv contains two genes (*Rv0654* and *Rv0913c*) encoding putative carotenoid oxygenases. Although the enzymatic activity of the *Rv0913c* encoded enzyme remains to be elucidated, we present data obtained in the present study (see summary of the substrates analyzed; Table 3) suggesting that the *Rv0654* encoded enzyme MtCCO is a carotenoid cleavage oxygenase novel with respect to the cleavage pattern, the conversion of aromatic carotenoids and its mycobacterial origin.

The identified cyclic products suggested that MtCCO can target two different sites in the same substrate (i.e. the C13-C14 and the C15-C15′ double bonds). Carotenoid oxygenases acting on bicyclic C_{40}-carotenoids mediate either a central cleavage at the C15-C15′ double bond, leading to two C_{20}-products (e.g. the animal BCO I [24–26] and the fungal CarX [27]) or an excentric cleavage at a different double bond, which results in two products that are different in chain length. The latter reaction was shown for the animal BCO II

Table 3. Summary of analyzed substrates. +, Cleaved; (+), only traces of the corresponding C_{20}- and C_{18}-products were observed; ND, cleavage not detected. Conversion of lycopene was only detected *in vivo*.

Substrate	Cleavage
Cholecalciferol	ND
Phylloquinone	ND
α-tocopherol	ND
Resveratrol	ND
β-apo-8′-carotenal	+
β-apo-10′-carotenal	+
β-apo-12′-carotenal	(+)
β-apo-14′-carotenal	ND
β-apo-15′-carotenal (retinal)	ND
β-apo-15′-carotenoic acid (retinoic acid)	ND
3-OH-β-apo-8′-carotenal	+
3-OH-β-apo-10′-carotenal	+
β-carotene	+
Zeaxanthin	+
Lutein	+
3,3′-dihydoxy-isorenieratene	+
Lycopene	+ (*in vivo*)

[29,30] and the plant CCD7 [35, 47] enzymes, which catalyze the cleavage of the C9-C10′ double bond of β-carotene leading to β-apo-10′-carotenal and β-ionone. The novelty of MtCCO is mirrored by its capability to act as a central, as well as an excentric cleavage enzyme. The considerable relative amounts of the corresponding products suggested that, at least in the case of lutein and 3,3′-dihydroxy-isorenieratene, none of these two activities is negligible (Table 2).

The expression of MtCCO in *E. coli* cells accumulating lycopene indicated a cleavage of carotenoids *in vivo*. However, the amounts of the products analyzed by HPLC were very low. Similar results were obtained from β-carotene- and zeaxanthin-accumulating cells (data not shown). The low cleavage activity in this *in vivo* system may be the result of the solubility of the enzyme, which impedes an access to the carotenoids accumulated in membranes, as assumed for the cyanobacterial carotenoid cleavage enzyme *Nostoc* carotenoid cleavage dioxygenase, which is localized in the soluble fraction of *Nostoc* cells and did not convert carotenoids in the corresponding accumulating *E. coli* strains [43].

The aromatic carotenoid isorenieratene (ϕ,ϕ-carotene; also named leprotene) and its hydroxylated derivatives are common mycobacterial pigments accumulated in several species [6,48,49]. Isorenieratene occurs also in some other actinomycetes; for example, *Streptomyces griseus* [50] and the coryneform bacterium *Brevibacterium linens* [51]. The conversion of 3,3′-dihydroxy-isorenieratene by MtCCO, as demonstrated in the present study, is a novel reaction. Indeed, MtCCO is the first enzyme shown to cleave aromatic carotenoids, and this activity may represent the function of orthologs in mycobacterial species accumulating these compounds.

Many mycobacterial species are known to accumulate carotenoids either in a light-independent manner (scotochromogens) or upon exposure to light (photochromogen) [52]. The synthesis of carotenoids in the photomorphogenic mycobacterium *M. aurum* is mediated by a gene cluster consisting of eight ORFs and organized in two operons [48,53]. Functional characterization of the constituents allowed the elucidation of the pathway via β-carotene down to isorenieratene [48], whereas the enzymes responsible for the hydroxylation leading to 3-monohydroxy- and 3,3′-dihydroxy-isorenieratene are still unknown. The enzymes involved in β-carotene formation are conserved in *M. marinum* [54]. On the basis of sequence similarity to the *M. marinum* phytoene synthase (CrtB) mediating the first commited step in carotenogenesis, the ORF *Rv3397c* encoded enzyme (accession number NP_217914) of *M. tuberculosis H37Rv* was identified as a phytoene synthase homolog [55]. However, sequence comparisons (not shown) reveal that this enzyme is rather related to a *S. griseus* putative squalene/phytoene synthase with unknown function (accession number AAG28701; 60% similarity) than to the authentic phytoene synthase from *S. griseus* (accession number AAG28701; 43% similarity) or *M. marinum* (accession number AAB71428; 39% similarity). This indicates that the *M. tuberculosis H37Rv* CrtB-homolog may catalyze a condensation reaction leading to an isoprenoid different from phytoene. This is further supported by the absence of genes coding for other enzymes in the carotenoid pathway. Taken together, genome analyses exclude a capability of *M. tuberculosis* to synthesize conventional colored carotenoids. However, there is still the possibility that *M. tuberculosis* synthesizes other unknown isoprenoid secondary metabolites, which may represent the natural MtCCO substrates.

The data reported in the present study suggest that *M. tuberculosis* may recruit carotenoids from its host to produce compounds required for normal growth. This speculation is supported by the occurrence of suitable carotenoid-substrates (i.e. β-carotene, lutein, zeaxanthin and lycopene) in human plasma and tissues [17]. In addition, the apocarotenoid substrate β-apo-10′-carotenal may also be present in lungs, as indicated by the expression pattern of the corresponding mammalian β-carotene cleaving enzyme BCO II [29,30]. Such a scenario would resemble the uptake of other

host lipids (i.e. fatty acids and cholesterol) and their utilization by this intracellular parasite [56,57]. The exploitation of the host resources may have allowed the reduction of the *M. tuberculosis* genome, by making its own biosynthetic capacities dispensable. Moreover, the activities of MtCCO may interfere with the carotenoid metabolism of the host cell and the produced retinoids/apocarotenoids may affect the immune response. It is striking that the ORF *Rv0655* occurring immediately downstream of the MtCCO gene (*Rv0654*) encodes a putative ribonucleotide ABC transporter ATP-binding protein, which may mediate the transport of these compounds.

Experimental procedures

Plasmid construction

The gene *Rv0654* was synthesized by Epoch Biolabs, Inc. (Missouri City, TX, USA) and cloned into a modified pBluescript II SK to yield pBSK-Myc1. *Rv0654* was then amplified with the primers MycI-A: 5′-GGAGGATCCAT GACCACCGCACAAGC-3′ and MycI-B: 5′-GAGCCC GGGAATTCGACTCACTATAGG-3′ using one unit of Phusion™ High-Fidelity DNA Polymerase (Finnzymes, Espo, Finland), in accordance with the manufacturer's instructions. The obtained product was purified using GFX™ PCR DNA and Gel Band Purification Kit (Amersham Biosciences, Piscataway, NJ, USA) and cloned into pBAD/THIO-TOPO® TA (Invitrogen, Paisley, UK) to yield pThio-Myc1 encoding MtCCO in fusion with thioredoxin. For the expression of glutathione *S*-transferase fusion protein, *Rv0654* was excised from pThio-Myc1 with *Bam*HI and *Sma*I. The fragment was then treated with T4-DNA polymerase and ligated into *Sma*I digested and dephosphorylated pGEX-5X-3 (Amersham Biosciences) to yield pGEX-5X-Myc1. The identity of the gene was verified by sequencing.

Protein expression and purification

The plasmid pGEX-5X-Myc1 was transformed into BL21(Tuner™DE3) *E. coli* cells (Novagen, Darmstadt, Germany) harbouring the plasmid pGro7 (Takara Bio Inc., Mobitec, Göttingen, Germany), which encodes the groES-groEL-chaperone system under the control of an arabinose-inducible promoter. Some 2.5 mL of overnight cultures of transformed cells were then inoculated into 50 mL of 2 × YT-medium containing arabinose (0.2%, w/v), grown at 28 °C until D_{600} of 0.5 was reached and induced with 0.2 mM isopropyl thio-β-D-glactoside. Cultures were then grown for 4 h at 28 °C, followed by 12 h at 20 °C. The fusion protein was purified using glutathione-sepharose 4B (Amersham Biosciences) and MtCCO was released by overnight treatment with the protease factor X_a in NaCl/P_i containing 0.1% Triton X-100 (v/v) at room temperature. Purification steps and protein expression were controlled by SDS/PAGE.

Enzymatic assays

Substrates were purified using thin-layer silica-gel plates (Merck, Darmstadt, Germany). Plates were developed with light petroleum/diethyl ether/acetone (40 : 10 : 10, v/v). Substrates were scraped off in dim daylight and eluted with acetone. Lutein and zeaxanthin were purified from spinach and *Synechocystis* sp. PCC 6803, respectively. Lycopene and β-carotene were purchased from Roth (Karlsruhe, Germany). 3,3′-dihydroxy-isorenieratene was synthesized according to Martin *et al.* [58], and apocarotenoids were kindly provided by BASF (Ludwigshafen, Germany). Enzyme assays were performed in a total volume of 200 μL as described previously [34] with some modifications. Some 50 μL of ethanolic substrate solution (200 μM) were mixed with 50 μL of ethanolic 4% octyl-β-glucoside solution, dried using a vacuum centrifuge and then resuspended in 100 μL of 2 × incubation buffer containing 2 mM Tris(2-carboxyethyl)phosphine hydrochloride, 0.6 mM $FeSO_4$ and 2 mg·mL^{-1} catalase (Sigma, Deisenhofen, Germany) in 200 mM Hepes-NaOH (pH 7.8). Purified MtCCO was then added to a final concentration of 50 ng·μL^{-1} for apocarotenoid assays or 300 ng·μL^{-1} for incubations with C_{40}-carotenoids, and assays were incubated for 2 and 4 h at 28 °C, respectively. The incubations were stopped by adding one volume of acetone and partitioned twice against two volumes of light petroleum/diethyl ether (1 : 4, v/v). Lipophilic supernatants were combined, dried and resolved in chloroform.

In vivo test

Carotenoid-accumulating *E. coli* TOP10 cells, harbouring the required biosynthetic genes from *Erwinia herbicola*, were transformed with pThio-Myc1 and the void plasmid pBAD-Thio. Overnight cultures of the obtained strains were inoculated into LB medium, grown at 28 °C until D_{600} of 0.5 was reached and induced with 0.2% arabinose. Cells were then harvested after 4 h and extracted using acetone/methanol (7 : 3, v/v). Extracts were then dried, resolved in chloroform and subjected to HPLC analyses.

Analytical methods

Substrates were quantified spectrophotometrically at their individual λ_{max} using extinction coefficients as given by Barua and Olson [31] or Davies [59]. Protein concentration was determined using the BioRad protein assay kit (BioRad, Hercules, CA, USA). A Waters system (Waters GmbH,

Eschborn, Germany) equipped with a photodiode array detector (model 2996) was employed for HPLC analyses performed using a YMC-Pack C_{30}-reversed phase column (250 × 4.6 mm inner diameter, 5 μm; YMC Europe, Schermbeck, Germany) with the solvent systems B: methanol/water/*t*-butylmethyl ether (50 : 45 : 5, v/v) and A: methanol/*t*-butylmethyl ether (500 : 500, v/v). The column was developed at a flow rate of 1 mL·min^{-1} with a linear gradient from 100% B to 43% B within 45 min, to 0% B within 1 min, then increasing the flow rate to 2 mL·min^{-1} within 1 min and maintaining these final conditions for another 14 min.

To determine the relative ratios of the C_{18}- and C_{20}-products, chromatograms were recorded as a MaxPlot (300–550 nm) using Empower Pro Software (Waters) allowing detection of peaks at their individual λ_{max}. The peaks of the two products were integrated and summed up to 100%. The relative ratio of each product was determined as the ratio of the corresponding peak surface.

LC-MS analyses were performed using a Thermo Finnigan LTQ mass spectrometer coupled to a Surveyor HPLC system consisting of a Surveyor Pump Plus, Surveyor PDA Plus and Surveyor Autosampler Plus (Thermo Electron, Waltham, MA, USA). Separations were carried out using a YMC-Pack C30-reversed phase column (150 × 3.0 mm inner diameter, 3 μm; YMC Europe) with the solvent system A: methanol/water/*t*-butylmethyl ether (50 : 45 : 5, v/v) and B: methanol/water/*t*-butylmethyl ether (27 : 3 : 70, v/v) with the water containing 0.1 g·L^{-1} ammonium acetate. The column was developed at a flow rate of 450 μL·min^{-1} with 90% A and 10% B for 5 min, to 5% A and 95% B within 10 min, then increasing the flow rate to 900 μL within 2 min and maintaining these final conditions for 5 min.

Products were identified by atmospheric pressure chemical ionization in positive mode. Nitrogen was used as sheath and auxiliary gas, which were set to 20 and 5 units, respectively. The source current was set to 5 μA and the capillary voltage was 49 V. Vaporizer and capillary temperatures were 225 and 175 °C, respectively.

Kinetic analysis

Initial measurements were carried out photometrically at 28 °C using a UV-2501PC spectrophotometer (Shimadzu Corp., Kyoto, Japan). As time linearity was observed over 6 min, the initial velocities were measured at 3.5 min. Enzymatic assays were performed with 0.1 μg·μL^{-1} purified MtCCO in 700 μL of incubation buffer at 28 °C. The reaction was started by adding the C_{30} and C_{27} substrates at final concentrations in the range 7–40 and 5–45 μM, respectively. Conversion was measured photometrically at the corresponding substrate absorption maxima. Kinetic parameters were determined using the GRAPHPAD PRISM 5.0 software (GraphPad Software Inc., San Diego, CA, USA).

Acknowledgements

This work was supported by the Deutsche Forschungsgemeinschaft (DFG) Grants AL892-1-3 and AL892-1-4, and by a grant to Dr Peter Beyer from the Bill & Melinda Gates Foundation as part of the Grand Challenges in Global Health Initiative. We are indebted to Dr Peter Beyer and Dr Ivan Paponov for valuable discussions.

References

1 Kaufmann SH (2001) How can immunology contribute to the control of tuberculosis? *Nat Rev Immunol* **1**, 20–30.
2 Russell DG (2001) *Mycobacterium tuberculosis*: here today, and here tomorrow. *Nat Rev Mol Cell Biol* **2**, 569–577.
3 Trimble WS & Grinstein S (2007) TB or not TB calcium regulation in mycobacterial survival. *Cell* **130**, 12–14.
4 Pieters J (2008) *Mycobacterium tuberculosis* and the macrophage: maintaining a balance. *Cell Host Microbe* **3**, 399–407.
5 Tobin DM & Ramakrishnan L (2008) Comparative pathogenesis of *Mycobacterium marinum* and *Mycobacterium tuberculosis*. *Cell Microbiol* **10**, 1027–1039.
6 Goodwin TW (1980) *The Biochemistry of the Carotenoids*. Vol. **I**, pp. 298–307. Chapmann and Hall, London.
7 Hirschberg J (2001) Carotinoid biosynthesis in flowering plants. *Curr Opin Plant Biol* **4**, 210–218.
8 Fraser PD & Bramley PM (2004) The biosynthesis and nutritional uses of carotenoids. *Prog Lipid Res* **43**, 228–265.
9 DellaPenna D & Pogson BJ (2006) Vitamin synthesis in plants: tocopherols and carotenoids. *Annu Rev Plant Biol* **57**, 711–738.
10 Harrison EH (2005) Mechanisms of digestion and absorption of dietry vitamin A. *Annu Rev Nutr* **25**, 87–103.
11 Blomhoff R & Blomhoff HK (2005) Overview of retinoid metabolism and function. *J Neurobiol* **66**, 606–630.
12 Moise AR, Noy N, Palczewski K & Blaner WS (2007) Delivery of retinoid-based therapies to target tissues. *Biochemistry* **46**, 4449–4458.
13 Spudich JL, Yang CS, Jung KH & Spudich EN (2000) Retinylidene proteins: structures and functions from archae to humans. *Annu Rev Cell Dev Biol* **16**, 365–392.
14 Ross SA, McCaffery PJ, Drager UC & De Luca LM (2000) Retinoids in embryonal development. *Physiol Rev* **80**, 1021–1054.
15 Duester G (2008) Retinoic acid synthesis and signalling during early organogenesis. *Cell* **134**, 921–931.

16 Mora JR, Iwata M & von Andrian UH (2008) Vitamin effects on the immune system: vitamins A and D take centre stage. *Nat Rev Immunol* **8**, 685–698.
17 Mein JR, Lian F & Wang XD (2008) Biological activity of lycopene metabolites: implications for cancer prevention. *Nutr Rev* **66**, 667–683.
18 Moise AR, von Lintig J & Palczewski K (2005) Related enyzymes solve evolutionarily recurrent problems in the metabolism of carotenoids. *Trends Plant Sci* **10**, 178–186.
19 Kloer DP & Schulz GE (2006) Structural and biological aspects of carotenoid cleavage. *Cell Mol Life Sci* **63**, 2291–2303.
20 Auldridge ME, McCarty DR & Klee HJ (2006) Plant caroteoid cleavage oxgenases and their apocarotenoid products. *Curr Opin Plant Biol* **9**, 315–321.
21 Walter MH, Floss DS & Strack D (2010) Apocarotenoids: hormones, mycorrhizal metabolites and aroma volatiles. *Planta* **232**, 1–17.
22 Kamoda S & Saburi Y (1993) Cloning, expression, and sequence anlysis of a lignostilbene-alpha, beta-dioxygenase gene from *Pseudomonas paucimobilis* TMY1009. *Biosci Biotechnol Biochem* **57**, 926–930.
23 Marasco EK & Schmidt-Dannert C (2008) Identification of bacterial carotenoid cleavage dioxygenase homologues that cleave the interphenyl alpha, beta double bond of stilbene derivatives via a monooxygenase reaction. *Chembiochem* **16**, 1450–1461.
24 von Lintig J & Vogt K (2000) Filling the gap in vitamin A research. Molecular identification of an enzyme cleaving beta-carotene to retinal. *J Biol Chem* **275**, 11915–11920.
25 Wyss A, Wirtz G, Woggon W, Brugger R, Wyss M, Friedlein A, Bachmann H & Hunziker W (2000) Cloning and expression of beta,beta-carotene 15,15′-dioxygenase. *Biochem Biophys Res Commun* **271**, 334–336.
26 Redmond TM, Gentleman S, Duncan T, Yu S, Wiggert B, Gantt E & Cunningham FX Jr (2001) Identification, expression, and substrate specificity of a mammalian beta-carotene 15,15′-dioxygenase. *J Biol Chem* **276**, 6560–6565.
27 Prado-Cabrero A, Scherzinger D, Avalos J & Al-Babili S (2007) Retinal biosynthesis in fungi: characterization of the carotenoid oxygenase CarX from *Fusarium fujikuroi*. *Eukaryot Cell* **4**, 650–657.
28 Estrada AF, Brefort T, Mengel C, Díaz-Sánchez V, Alder A, Al-Babili S & Avalos J (2009) *Ustilago maydis* accumulates beta-carotene at levels determined by a retinal-forming carotenoid oxygenase. *Fungal Genet Biol* **46**, 803–813.
29 Kiefer C, Hessel S, Lampert JM, Vogt K, Lederer MO, Breithaupt DE & von Lintig J (2001) Identification and characterization of a mammalian enzyme catalyzing the asymmetric oxidative cleavage of provitamin A. *J Biol Chem* **276**, 14110–14116.
30 Hu KQ, Liu C, Ernst H, Krinsky NI, Russell RM & Wang XD (2006) The biochemical characterization of ferret carotene-9′,10′-monooxygenase catalyzing cleavage of carotenoids *in vitro* and *in vivo*. *J Biol Chem* **281**, 19327–19338.
31 Barua AB & Olson JA (2000) beta-carotene is converted primarily to retinoids in rats *in vivo*. *J Nutr* **130**, 1996–2001.
32 Ruch S, Beyer P, Ernst H & Al-Babili S (2005) Retinal biosynthesis in Eubacteria: *in vitro* characterization of a novel carotenoid oxygenase from *Synechocystis* sp. PCC 6803. *Mol Microbiol* **55**, 1015–1024.
33 Scherzinger D, Ruch S, Kloer DP, Wilde A & Al-Babili S (2006) Retinal is formed from apo-carotenoids in *Nostoc* sp. PCC7120: in vitro characterization of an apo-carotenoid oxygenase. *Biochem J* **398**, 361–369.
34 Alder A, Holdermann I, Beyer P & Al-Babili S (2008) Carotenoid oxygenases involved in plant branching catalyse a highly specific conserved apocarotenoid cleavage reaction. *Biochem J* **416**, 289–296.
35 Schwartz SH, Qin X & Loewen MC (2004) The biochemical characterization of two carotenoid cleavage enzymes from *Arabidopsis* indicates that a carotenoid-derived compound inhibits lateral branching. *J Biol Chem* **279**, 46940–46945.
36 Gomez-Roldan V, Fermas S, Brewer PB, Puech-Pages V, Dun EA, Pillot JP, Letisse F, Matusova R, Danoun S, Portais JC *et al*. (2008) Strigolactone inhibition of shoot branching. *Nature* **455**, 189–194.
37 Umehara M, Hanada A, Yoshida S, Akiyama K, Arite T, Takeda-Kamiya N, Magome H, Kamiya Y, Shirasu K, Yoneyama K *et al*. (2008) Inhibition of shoot branching by new terpenoid plant hormones. *Nature* **455**, 195–200.
38 Leyser O (2008) Strigolactones and shoot branching: a new trick for a young dog. *Dev Cell* **15**, 337–338.
39 Akiyama K & Hayashi H (2008) Plastid-derived strigolactones show the way to roots for symbionts and parasites. *New Phytol* **178**, 695–698.
40 Bouwmeester HJ, Roux C, Lopez-Raez JA & Becard G (2007) Rhizosphere communication of plants, parasitic plants and AM fungi. *Trends Plant Sci* **12**, 224–230.
41 Stinear TP, Seemann T, Harrison PF, Jenkin GA, Davies JK, Johnson PD, Abdellah Z, Arrowsmith C, Chillingworth T, Churcher C *et al*. (2008) Insights from the complete genome sequence of *Mycobacterium marinum* on the evolution of *Mycobacterium tuberculosis*. *Genome Res* **18**, 729–741.
42 Cole ST, Brosch R, Parkhill J, Garnier T, Churcher C, Harris D, Gordon SV, Eiglmeier K, Gas S, Barry CE *et al*. (1998) Deciphering the biology of *Mycobacterium tuberculosis* from the complete genome sequence. *Nature* **393**, 537–544.
43 Scherzinger D & Al-Babili S (2008) *In vitro* characterization of a carotenoid cleavage dioxygenase from

Nostoc sp. PCC 7120 reveals a novel cleavage pattern, cytosolic localization and induction by highlight. *Mol Microbiol* **69**, 231–244.
44 Kloer DP, Ruch S, Al-Babili S, Beyer P & Schulz GE (2005) The structure of a retinal-forming carotenoid oxygenase. *Science* **308**, 267–269.
45 Ilg A, Beyer P & Al-Babili S (2009) Characterization of the rice carotenoid cleavage dioxygenase 1 reveals a novel route for geranial biosynthesis. *FEBS J* **276**, 736–747.
46 Miller CD, Hall K, Liang YN, Nieman K, Sorensen D, Issa B, Anderson AJ & Sims RC (2004) Isolation and characterization of polycyclic aromatic hydrocarbon-degrading *Mycobacterium* isolates from soil. *Microb Ecol* **48**, 230–238.
47 Booker J, Auldridge M, Wills S, McCarty D, Klee H & Leyser O (2004) MAX3/CCD7 is a carotenoid cleavage dioxygenase required for the synthesis of a novel plant signaling molecule. *Curr Biol* **14**, 1232–1238.
48 Viveiros M, Krubasik P, Sandmann G & Houssaini-Iraqui M (2000) Structural and functional analysis of the gene cluster encoding carotenoid biosynthesis in *Mycobacterium aurum* A+. *FEMS Microbiol Lett* **187**, 95–101.
49 Provvedi R, Kocíncová D, Donà V, Euphrasie D, Daffé M, Etienne G, Manganelli R & Reyrat JM (2008) SigF controls carotenoid pigment production and affects transformation efficiency and hydrogen peroxide sensitivity in *Mycobacterium smegmatis*. *J Bacteriol* 7859–7863.
50 Krügel H, Krubasik P, Weber K, Saluz HP & Sandmann G (1999) Functional analysis of genes from *Streptomyces griseus* involved in the synthesis of isorenieratene, a carotenoid with aromatic end groups, revealed a novel type of carotenoid desaturase. *Biochim Biophys Acta* **1439**, 57–64.
51 Krubasik P & Sandmann G (2000) A carotenogenic gene cluster from *Brevibacterium linens* with novel lycopene cyclase genes involved in the synthesis of aromatic carotenoids. *Mol Gen Genet* **263**, 423–432.
52 Barksdale L & Kim KS (1977) Mycobacterium. *Bacteriol Rev* **41**, 217–372.
53 Houssaini-Iraqui M, Lazraq MH, Clavel-Sérès S, Rastogi N & David HL (1992) Cloning and expression of *Mycobacterium aurum* carotenogenesis genes in *Mycobacterium smegmatis*. *FEMS Microbiol Lett* **69**, 239–244.
54 Gao L, Groger R, Cox JS, Beverley SM, Lawson EH & Brown EJ (2003) Transposon mutagenesis of *Mycobacterium marinum* identifies a locus linking pigmentation and intracellular survival. *Infect Immun* **71**, 922–929.
55 Ramakrishnan L, Tran HT, Federspiel NA & Falkow S (1997) A crtB homolog essential for photochromogenicity in *Mycobacterium marinum*: isolation, characterization & gene disruption via homologous recombination. *J Bacteriol* **179**, 5862–5868.
56 Ehrt S & Schnappinger D (2007) *Mycobacterium tuberculosis* virulence: lipids inside and out. *Nat Med* **13**, 284–285.
57 Pandey AK & Sassetti CM (2008) Mycobacterial persistence requires the utilization of host cholesterol. *Proc Natl Acad Sci U S A* **105**, 4376–4380.
58 Martin HD, Kock S, Scherrers R, Lutter K, Wagener T, Hundsdörfer C, Frixel S, Schaper K, Ernst H, Schrader W *et al.* (2008) 3,3′-Dihydroxyisorenieratene, a natural carotenoid with superior antioxidant and photoprotective properties. *Angew Chem* **120**, 1–6.
59 Davies BH (1976) Carotenoids In *Chemistry and Biochemistry of Plant Pigments*, 2nd edn, Vol. **2** (Goodwin TW ed.), pp. 150–153. Academic Press, London.
60 Clamp M, Cuff J, Searle SM & Barton GJ (2004) The Jalview Java alignment editor. *Bioinformatics* **20**, 426–427.
61 Tamura K, Dudley J, Nei M & Kumar S (2007) MEGA4: Molecular Evolutionary Genetics Analysis (MEGA) software version 4.0. *Mol Biol Evol* **24**, 1596–1599.

Supporting information

The following supplementary material is available:
Fig. S1. Sequence comparison of MtCCO with the *Nostoc* carotenoid cleavage dioxygenase (NosCCD) [59,60].
Fig. S2. Coomassie-stained SDS/PAGE gel of MtCCO purification fractions.
Fig. S3. Mean velocity (s^{-1}) of three independent kinetic measurements of recombinant MtCCO cleaving β-apo-8′-carotenal.
Fig. S4. Phylogenetic relationship of selected bacterial members of the carotenoid oxygenase family [Neighbor-joining (NJ) method].
Table S1. Data of three independent kinetic measurements of recombinant MtCCO cleaving β-apo-8′-carotenal.

This supplementary material can be found in the online version of this article.

Please note: As a service to our authors and readers, this journal provides supporting information supplied by the authors. Such materials are peer-reviewed and may be re-organized for online delivery, but are not copy-edited or typeset. Technical support issues arising from supporting information (other than missing files) should be addressed to the authors.